11-17-2005

Progress towards terahertz acoustic phonon generation in doping superlattices

Thomas E. Wilson
Marshall University, wilsont@marshall.edu

Recommended Citation

Wilson TE. "Progress towards terahertz acoustic phonon generation in doping superlattices." In proceedings of SPIE 6010, Infrared to Terahertz Technologies for Health and the Environment, Belyanin A, Drezek R, Gmachl C, editors, Vol. 6010, 601007, (2005)

Progress towards terahertz acoustic phonon generation in doping superlattices

Thomas E. Wilson[*a]
[a]Department of Physics, Marshall University, One John Marshall Drive, Huntington, WV 25755-2570

ABSTRACT

Progress is described in experiments to generate coherent terahertz acoustic phonons in silicon doping superlattices by the resonant absorption of nanosecond-pulsed far-infrared laser radiation. Future experiments are proposed that would use the superlattice as a transducer in a terahertz cryogenic acoustic reflection microscope with sub-nanometer resolution.

Keywords: doping superlattice, terahertz, acoustic, phonon, superconducting bolometer, cryogenic, acoustic microscope

1. INTRODUCTION

The optical generation of coherent, monochromatic acoustic phonons has been a long-standing goal in solid state physics. The generation and detection of longitudinal acoustic (LA) phonons with frequency up to 114 gigahertz (GHz) was accomplished through the electromagnetic surface excitation of piezoelectric crystals[1] in completely filled TM cavities. Unfortunately, reported results on the generation of terahertz (THz) transverse acoustic (TA) phonons in quartz through piezoelectric surface excitation with far-infrared laser light have proven not to be repeatable.[2] More recently however, progress has been made using the elegant technique of picosecond ultrasonics (PU) to generate and detect coherent LA phonons, with frequencies exceeding 400 GHz, acoustic intensities exceeding 100 W/cm^2 with corresponding strain amplitudes on the order of 10^{-4}, in solid thin films near room temperature.[3] Furthermore, it has also been reported that it is possible to generate coherent pulses of longitudinal acoustic phonons in a gallium arsenide/aluminum arsenide compositional superlattice by femtosecond laser excitation when the excitation energy matches the E1-HH1 transition in the superlattice[4]. We are currently investigating a complementary technique[5], that of the direct electromagnetic generation of coherent high-frequency monochromatic acoustic phonons in silicon doping superlattices (DSL) by a high peak-power, cavity-dumped, far-infrared (FIR) laser radiation. The latter has the potential to produce intense pulses of high-frequency narrow-bandwidth coherent acoustic phonons of either polarization.

Future applications include using the phonon-generating superlattice as a terahertz acoustic transducer in a cryogenic reflection acoustic microscope and with low-temperature helium-4 as the coupling fluid. State-of-the-art acoustic microscopes have a maximum resolution in the range of 20-nm and use sound waves with frequencies as high as 15-GHz[6]. We propose to improve this resolution to less than a nanometer by using the terahertz frequencies of the resonantly excited doping superlattice. Terahertz acoustic imaging with sub-nanometer resolution, by providing an additional image contrast mechanism (elastic properties), could be expected to provide a tool for the characterization of nanomaterials and nanoelectronic devices, and potentially for acoustic cryo-microscopy of biological samples.

[*] wilsont@marshall.edu; phone 1 304 696-2752; fax 1 304 696-3243

Infrared to Terahertz Technologies for Health and the Environment,
edited by Alexey A. Belyanin, Rebekah A. Drezek, Claire F. Gmachl, Proc. of SPIE
Vol. 6010, 601007, (2005) · 0277-786X/05/$15 · doi: 10.1117/12.630201

2. THEORY

Modulation-doped compositional superlattices and *nipi* doping superlattices have been the objects of intense theoretical and experimental study in the past several decades[7]. A number of authors[5] have studied the effects, on the lattice dynamical properties of an otherwise homogeneous semiconductor, stemming from impurity charges associated with a microstructured one-dimensional periodic *n* and *p*-doping sequence, a so-called *nipi* doping superlattice. The phonon dispersion relation is nearly unchanged, as one might expect from a concentration of 10^{-3} impurity atoms or even less. The periodic space charge resulting from the doping superstructure, however, is the origin of a unique feature: LA or TA acoustic phonons, with wavevectors corresponding to odd multiples of the smallest reciprocal superlattice vector, may be directly excited by electromagnetic fields of the corresponding frequency with reasonable conversion efficiency. The frequency of the generated phonons is simply given by

$$\nu = s / d \quad ,$$

where *s* and *d* are the phase velocity for LA phonons and the superlattice period, respectively.

LA or TA phonons couple to electric fields normal or parallel to the superlattice layers, respectively. We note that, for our purposes, the *nipi* superlattice is preferred over a modulation-doped compositional superlattice because, in the case of the former, the splittings of the back-folded zone-center frequencies are small. One would therefore expect little conversion of the traveling wave into a standing wave by the Bragg scattering of the folded-zone center phonons.[8] The conversion efficiency, ξ, defined as the ratio of the generated acoustic energy to the energy of the incident electromagnetic wave, is given by equation (1) (cgs units) below, where *a* is the host lattice constant, $n_D^{(2)}$ is the two-dimensional doping concentration, κ_0 is the dielectric constant, *M* is the atomic mass, *d* is the superlattice period, *c* is the speed of light, *s* is the longitudinal phonon velocity, *N* is the number of superlattice periods, and $r \equiv (d/a)$, is the enlarged unit cell:

$$\xi \cong \left[\frac{\left(4\pi e^2 a^2 (n_D^{(2)})^2 (adN^2)\right)}{(\kappa_0 M d r)(cs\sqrt{\kappa_0})} \right] \qquad \textbf{(1)}$$

The upper limit to the two-dimensional (donor or acceptor) doping concentration is determined by the condition that there be an effective bandgap. The limiting doping concentration follows from equations (1) and (8) in Dohler[9], and is given in equation (3) below:

$$n_D^{(2)} \cong \left[\frac{\left(2E_g \kappa_0\right)}{(\pi d e^2)} \right] \quad , \qquad \textbf{(2)}$$

where E_g is the host bandgap. At this doping level, the thin sheets of acceptors and donors are degenerate and there will be no carrier freeze out at liquid helium temperatures.[10] In its ground state, the sample thus consists of alternately positively and negatively charged sheets of ions. Care must be taken to insure that the sample has a closely balanced dopant concentration.

As an example, we consider a silicon (Si) superlattice consisting of N periods, with a period of length d = 3.45 x 10^{-6} cm, and with individual layers having a two-dimensional doping concentration $n_D^{(2)}$ = 1.7x 10^{13} cm^{-2}. The conversion efficiency ξ of this superlattice, in terms of the number of superlattice periods N, is readily found from Equation (1): ξ = 4.75 x 10^{-11} N^2. For instance, for a structure consisting of 500 periods, ξ = 1.2 x 10^{-5}. The period chosen matches the LA phonon wavelength in silicon for 245.5-GHz (1.22–mm), a particularly strong far-infrared laser line produced by the $^{13}CH_3F$ gain medium (below). The corresponding phonon strain amplitude is on the order 10^{-6}.

In order to protect the sensitive superconducting bolometer detector from the intense FIR laser radiation, we use a small-period metallic grating coupler[11]; i.e., heat pulse generation in bolometers exposed to intense FIR laser pulses has been observed previously[2]. Broadband phonon generation might also be expected, in the absence of such a grating-coupling scheme, to result both from multi-phonon-[12] and defect-induced-[13] absorption in the substrate. The grating coupler has drawn considerable interest in recent years since it has been shown to significantly improve the intersubband absorption in multiple quantum-well infrared photodetectors under normally incident illumination.[11] The grating coupler converts normally incident plane wave radiation, into an evanescent surface wave with a large electric field component perpendicular to the interface. The decay length δ of the first-order diffracted evanescent ($p/(\lambda/n) < 1$) field of the grating-coupler is given by Equation (7) of Reference 11:

$$\delta \cong \left[\frac{p}{2\pi\sqrt{1-(np/\lambda)^2}} \right], \qquad \textbf{(3)}$$

where p is the grating period and λ/n is the optical wavelength of the FIR in the DSL. For a given δ, equation (3) may be inverted to find the optimum grating period p. Ideally, one would choose the decay length to match the DSL thickness; in our case, the overall DSL thickness (14 layers x 34.5-nm period) corresponds to a δ~0.5-μm. However, we have used a grating period of p~10-μm, resulting in a decay length of δ~1.6-μm, slightly larger than the overall superlattice thickness. The larger p was chosen due to constraints imposed by our photolithography system. (n = 3.41 for silicon at 246-GHz). Niobium was used as the grating material because of its small surface resistance (i.e., low FIR absorption) below its superconducting transition temperature[14].

The spectral and polarization characteristics of the generated coherent acoustic phonons will be studied using Si:B piezo phonon spectroscopy[15]. The phonons, generated in the DSL, will propagate ballistically through a lightly boron-doped Si substrate and will be detected by a granular aluminum superconducting bolometer[16] located on the rear sample face. The sample, cooled by immersion in liquid helium by means of a cryostat with optical access, is uniformly stressed at levels up to several kBar by a stress apparatus suitable for use in low-temperature cryostats[17]. Along symmetry directions in Si:B, the stress-dependent energy level splitting of the boron acceptor's ground-state Kramer's doublets is known. The bolometer signal will drop sharply when the energy difference between the stress-split levels matches the phonon energy. Measurements of the phonon transmission as a function of the applied stress will yield the phonon spectrum. Furthermore, the spectral content of TA and LA phonons may be studied independently by gating the detector signal at the corresponding phonon time-of-flight across the substrate. The spectrometer resolution, under the conditions of the proposed experimental arrangement, is typically 5 GHz; this is of the same order as the predicted phonon linewidth resulting from a 100-period thick DSL. The temporal resolution, determined by the bolometer response, is typically of order 10 ns (Figure 4). We will generate and detect phonons at a number of discrete frequencies, ranging

from 0.25 to 1.0 THz, by using samples with different DSL period and corresponding FIR laser excitation wavelength. Measurements of the phonon spectral width and the relative conversion efficiency of electromagnetic to acoustic power will be compared to theory.

3. EXPERIMENT / PRELIMINARY RESULTS

3.1 The far-infrared laser

Strong pulsed lasing action at 1.22-mm was first reported by Hacker *et al*[18] in a $^{13}CH_3F$ mirrorless waveguide laser., optically-pumped by the 9P32 line of a TEA CO_2 laser. As a source of intense ultrashort (~nanosecond) pulses of far-infrared laser radiation suitable for this experiment, we use our[19] cavity-dumped optical laser resonator, modified for use at 1.22-mm. The laser resonator schematic diagram is depicted in Figure 1.

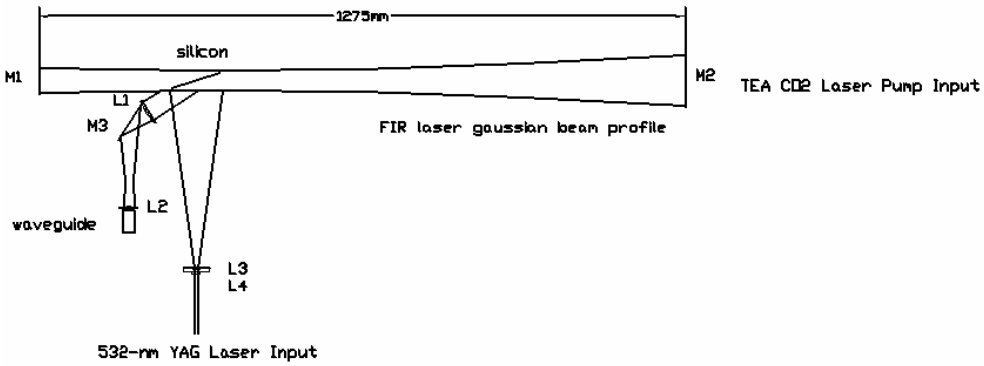

Figure 1. *FIR laser resonator schematic diagram. M1*: 10-cm diameter Au-coated concave copper mirror, radius of curvature 845 mm; *M2*: 10-cm diameter Au-coated concave copper mirror, radius of curvature 1275 mm; *Silicon*: {100) float-zone, double-sided polished, 100-mm diameter x 0.5 mm, 7000 Ohm-cm resistivity; *L1, L2*, plano-convex TPX lens, 159-mm and 105-mm focal length, respectively; *M3*: 75-mm diameter flat Au-coated Pyrex mirror; *L3*: 50-mm diameter, -100 mm focal length plano-concave BK7 spherical lens, visible AR coating; *L4*: -40 mm focal length cylindrical BK7 lens. Not shown: modified *Gentec DD-250* TEA CO_2 pumping laser (focused TEA laser radiation enters through 2-mm coupling hole in *M2*), *Spectra-Physics GCR-150* frequency-doubled YAG laser output entering through *L4*. The FIR laser output is coupled into a segmented 246-GHz corrugated waveguide.

Our technique for cavity-dumping by the optical-switching of an intra-cavity intrinsic silicon wafer, oriented at the Brewster angle to the circulating p-polarized far-infrared radiation, through the absorption of above bandgap radiation, has also been used elsewhere[20]. The risetime of the output pulse is typically on the order of a nanosecond and the pulsewidth corresponds to the roundtrip time of the circulating far-infrared radiation. Recent improvements to the laser have included: (1) an in-situ mode-matching Newtonian telescope, employing custom TPX lens, to couple the output into a 246-GHz corrugated waveguide[21] for beam transport (2) a recycling cryogenic absorption pump for the isotopic methyl fluoride gain medium. The laser routinely produces single-longitudinal mode pulsed output in peak powers of 25-kW (measured by a *Coherent Molectron*[22] *J25* pyroelectric joulemeter), 6-ns pulsewidth (measured by a *Coherent*

Figure 2. 1.22-mm cavity-dumped FIR (25kW) output and 532-nm switching radiation

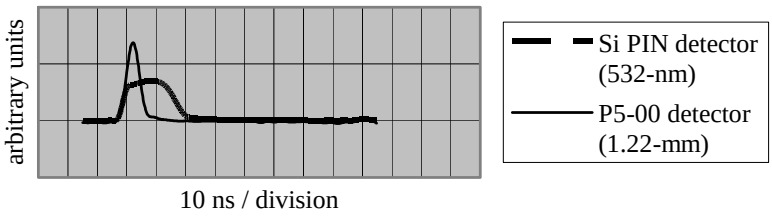

Molectron P5-00 pyroelectric detector) at a 10 pps repetition rate. FIR laser output is also available at other wavelengths, for instance at 496-micron, in CH_3F pumped by the 9P20 line. A typical output pulse is shown in Figure 2.

3.2 Granular aluminum bolometer and thin film patterning

The resonantly excited phonons not scattered by the boron acceptors will ordinarily propagate ballistically across the Si:B substrate and be detected on the opposite face by a superconducting granular aluminum bolometer[23]. Superconducting bolometers of this ilk typically have a phonon power detection threshold on the order of ~10^{-8} W without integration[2]. Our bolometers are 100-nm thick, 10 micron x 20 micron granular aluminum links that span the gap between millimeter-square chromium/gold contact pads. We fabricate the granular aluminum bolometers and niobium grating couplers, at the University of Delaware ECE Cleanroom, using a lift-off process with image-reversal lithography employing *AZ 5214 E* photoresist and *AZ Developer*, as partially described in the literature[24]. (The overall image-reversal process recipe characterization is nearly completed.) We have found it imperative to use *AZ Developer* since, unlike most positive photoresist developers; it does not etch aluminum (see Figure 5). We expose the silicon die on a *Karl Suss MJB3* mask aligner through chromium soda-lime photomasks, supplied by *Adtek Photomasks, Inc*, and designed with *L-Edit* software[25]. We use a *Discovery 18* load-lock dual-target DC-magnetron sputter deposition system[26] retrofitted with an oxygen lecture bottle and a precision leak valve arrangement. Starting from a base pressure of 1 microTorr, granular aluminum is sputtered for 80-seconds at 400-W in an 8.5 mTorr argon plasma with an oxygen partial pressure of 170 microTorr. To prevent oxidation of the granular aluminum surface during subsequent processing, a thin (5-nm) palladium film is sputtered, from a second target, on top of the granular aluminum, prior to breaking vacuum. Under these deposition conditions, it is found that that the granular aluminum/palladium bilayer possesses a room temperature resistivity in the range of 25 to 50 microOhm-cm and a corresponding superconducting transition temperature near 1.76-K. Furthermore, the palladium coating consistently results in reliable electrical connection to the overlying chromium/gold contacts – a new finding. The bolometer is cooled by immersion in He II by means of a cryostat with optical access. A constant temperature is maintained through pumping on the helium and controlling its vapor pressure with a regulator. This technique allows the selection of a fixed temperature from 1.4 K to 2.2 K with a constancy of better than 0.002 K, much less than the width of the superconducting transition. Figure 3 displays a recent four-point probe measurement of the superconducting transition of a U-Delaware fabricated granular aluminum/palladium bilayer. Figure 4 shows the recent test of a larger granular aluminum bolometer, fabricated earlier by shadow-mask evaporation in the laboratory of Dr. Werner Dietsche at MPI-Stuttgart. Figure 4 displays the arrival of a

heat pulse generated by on the front surface of a Si:B sample (with no doping superlattice), at the expected time-of-flight for LA phonons.

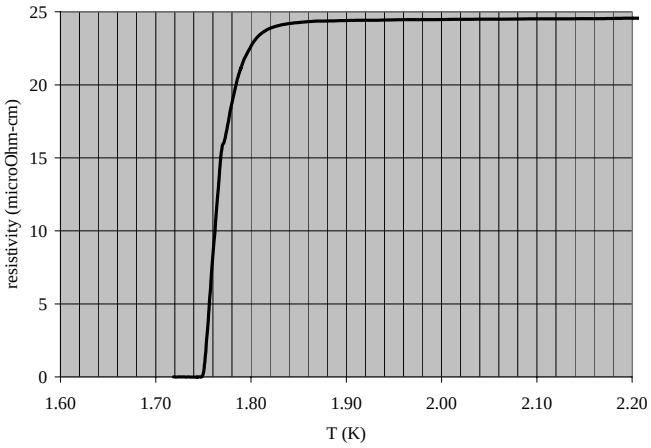

Figure 3: Four-point probe measurement of resistivity versus temperature for a sputtered granular aluminum/palladium bilayer. Temperature computed via helium vapour pressure according to the International Temperature Scale of 1990[27].

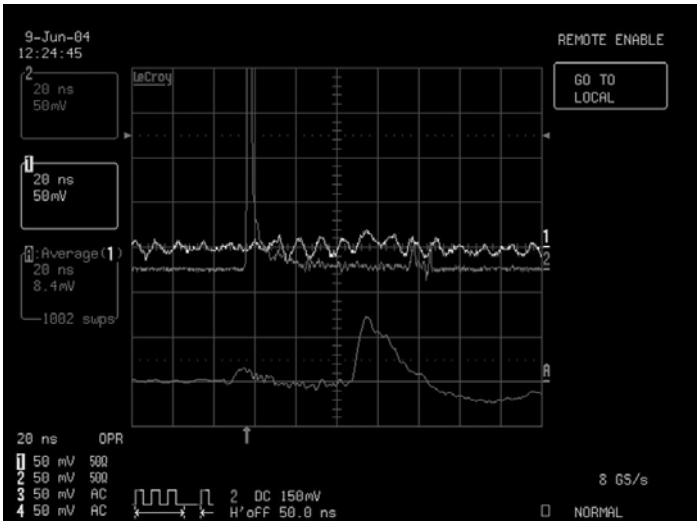

Figure 4: Granular aluminum bolometer response (second pulse on lowest trace) to heat pulse produced on front surface of an aluminum-coated {100} Si:B sample by 300-W mini-YAG laser irradiation (upper trace). The first pulse on the lowest trace corresponds to scattered light striking the bolometer. The second pulse on the lowest trace

corresponds to the time-of-flight (60-ns) for LA phonons in 0.5-mm thick silicon. A broadband impedance mini-transformer (16:1) positioned near the sample in the helium bath was used to match the 3-Ohm bolometer to 50-Ohm miniature coaxial cable.

We estimate the expected signal-to-noise ratio for the DSL phonon generation experiment as follows. For a DLS sample with 14 periods (one of our samples), the conversion efficiency ξ is 9.2 x 10^{-9}. The grating coupling efficiency, defined as the ratio of the total energy density associated with the component of the electric field of the FIR evanescent wave normal to the surface, to the energy density of the linearly polarized incident FIR wave, is estimated as 0.80. If one assumes 10-kW of FIR laser power incident upon the DSL, the expected phonon power arriving at the bolometer is 7.4 x 10^{-5} W, well above the threshold of detection.

The experiment awaits further bolometer fabrication development. It was observed that *AZ 351* developer etched the granular aluminum/palladium bilayer during the subsequent deposition of the contact pads. Work is in progress to develop an image-reversal process (for more consistent lift-off results) using the *AZ Developer* instead of the *AZ 351*.

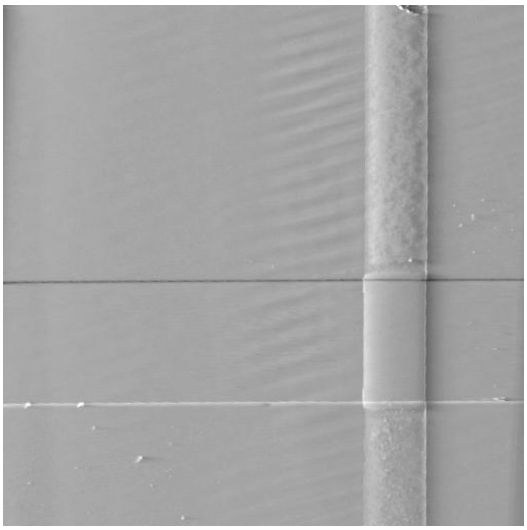

Figure 5: An atomic force microscope image of a 10 micron x 20 micron x 80-nm thick granular aluminum/palladium bilayer (spanning two larger chromium/gold contacts). Notice the roughness as a result of the etching of the aluminum (under the contacts) from the use of *AZ 351* developer during the subsequent processing of the contacts. Such etching prevents the bolometer from becoming superconducting.

3.3 Piezo phonon spectroscopy

The experimental method to be used for measuring phonon emission spectra using the Si:B spectrometer is described in the literature[28]. In the Si:B piezo phonon spectrometer, the boron acceptor ground state, consisting of a quartet, is split into two Kramers doublets by applied stress. Phonons are resonantly scattered by the acceptors when the phonon energy matches the difference in the energy levels of the doublets. For stress applied along the [100], [1101 and [111]

directions, the energy level splitting in Si:B, as a function of stress, is known. For example, the ground state splitting energy E as a function of stress X along a [100] direction is given by:

$$E = (392\ GHz/kBar)\ X \qquad (4)$$

The resonant scattering rate and linewidth, as a function of the splitting energy, acceptor concentration and temperature, are also known. For instance, near 250 GHz, the linewidth is ~5 GHz. The spectrum of any TA or LA phonons generated by the superlattice can be obtained by monitoring the transmitted phonon signal, received at the bolometer at the back face of the sample, as a function of stress applied in a direction normal to the propagating phonons. A significant drop in transmission should occur when the phonon energy matches the stress-split level separation. In addition, the spectral content of TA and LA phonons may be analyzed separately by gating the detector at the corresponding phonon time of flight. The time-dependent bolometer voltage can be numerically de-convoluted to obtain the time-dependent absorbed phonon flux.[16]

To prepare die for the stress apparatus, the wafer is first diced into 12-mm x 16-mm platelets and the thin films are patterned on a 2 x 2 array and then subsequently diced into 5-mm x 7-mm samples. The top and bottom

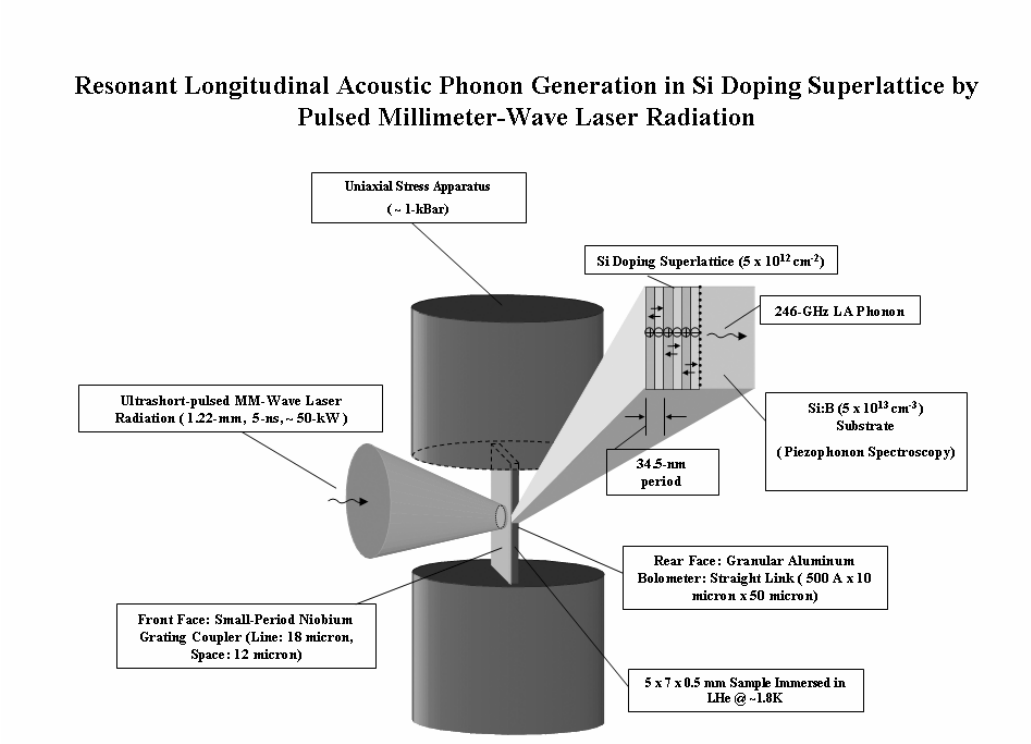

Figure 6: Schematic Diagram for Experimental Arrangement for Phonon Generation in Silicon Doping Superlattice by Pulsed Far-Infrared Laser Radiation

surfaces of the samples are lapped parallel to one another on a glass plate using a custom lapping fixture[29]. Flatness can be verified using an optical test jig based upon a design by Viertl[30]. The pistons of the stress apparatus are similarly

lapped and adjusted for parallelism. Parallel alignment of the pistons is accomplished by placing a small commercial gauge block between the pistons and then tightening the piston's alignment screws with a small torque wrench. Parallelism is readily verified by viewing, with crossed polarizers, the strain field of one of an identically-lapped (using the same lapping jig) fused quartz platelet, positioned between the pistons of the apparatus. When the pistons are parallel, the strain field of the quartz is uniform.

3.4 Summary

To summarize, the unique source of intense ultra-short pulsed THz (and sub-THz) laser radiation including corrugated-waveguide output coupling for convenient beam transport, the doping superlattice samples, a vapour-pressure regulated liquid helium cryostat, the uniaxial stress apparatus, and the bolometer signal recovery electronics, are all available and functional. The only remaining task before beginning the phonon generation experiment is to complete the bolometer fabrication work on the rear face of the DSL samples using image-reversal lithography with *AZ5214 E* photoresist and *AZ Developer*. The phonon generation experiments will follow immediately thereafter. Figure 6 shows the overall experimental arrangement.

4. FUTURE APPLICATION – THZ CRYOGENIC ACOUSTIC MICROSCOPE

4.1 Background

After phonon generation by our technique is established, we would like to purse the development of a cryogenic THz acoustic microscope by the following experiments: (1) the coherent detection of an electromagnetic echo produced in the superlattice from a specularly reflected phonon pulse at the rear surface of the substrate, immersed in 2-K liquid helium (2) the coherent detection of an electromagnetic echo produced in the superlattice from returning coherent phonons that have first propagated across the silicon interface into low temperature (0.150-K) liquid helium-4, and then reflect from a piezomotor-driven sapphire[31] phonon mirror also immersed in the liquid helium bath (3) the fabrication of an acoustic microlens coated with the phonon anti-reflection multilayer in order to focus the phonon beam in the liquid helium bath to a nanometer beamwaist.

The previous highest operating transducer frequency for a cryogenic acoustic microscope has been near 15 GHz. In this frequency regime (15-GHz), three-phonon decay processes have been shown to result in a depletion of the focused beam and to severely impact the signal to noise ratio.[32] However, above 209 GHz, sound attenuation and nonlinearity in low-temperature (<150 mK) helium do not appear to be limiting factors and mean free paths on the order of cm have been measured[33]. An acoustic microscope operating above 209 GHz, with a fast acoustic lens impedance-matched to liquid helium-4 (using a ^{3}He one-shot cryostat or a dilution refrigerator) as the coupling fluid, could be expected to possess a resolution of less than a nanometer – a major advance.

4.2 Coherent detection of electromagnetic echo

As the first experiment along the path to the development of a THz cryogenic acoustic microscope, the coherent nature of the generated phonons could be verified in a pulse-echo experiment with phonons remaining within the DSL

substrate immersed in a simple 2-K liquid helium cryostat. A phonon pulse, upon returning to the DSL after undergoing specular reflection (see discussion below) at the rear sample face, will generate an electromagnetic echo pulse which will be coherently detected. The coherence of the phonons in this context refers to the phonons, in the small volume, having a common propagation velocity, wavevector, and phase. For an optimal detection signal in the pulse-echo experiment, incident acoustic waves must have a wavefront parallel within a part of a wavelength to the DSL surface in order to get no phase cancellation in the mean value of the produced electric field. The thick, superpolished rear face of the substrate will satisfy parallelism and flatness conditions[34] for an acoustic wavelength on the order of tens of nanometers. The echo pulse would be coherently detected and captured on a fast (1-GHz bandwidth) digitizing oscilloscope. The phonon linewidth would be extracted by deconvolving the instrumental linewidth from the Fourier transform of the digitized echo pulse.

Coherent detection of the electromagnetic echo would be employed using a room-temperature Schottky-barrier diode mixer, with an NEP of 10^{-19} W/Hz$^{1/2}$, in a waveguide-based monolithic heterodyne receiver using the tripled output of a Gunn oscillator as the local oscillator (LO). The LO could provide up to 2 mW of cw power. A complete waveguide-based receiver at 245.5 GHz, containing a conventional mixer, the LO and the IF processing electronics, is commercially available.[35] We estimate the expected SNR as follows. The one-way conversion efficiency ξ of a DSL with period 34.5-nm and a maximum two-dimensional doping concentration of $n_D^{(2)} = 1.7 \times 10^{13}$ cm^2, expressed in terms of the number of periods N, is 4.7×10^{-11} N^2. Assuming a 50% grating coupling efficiency, a *50%* beamsplitter for the laser radiation, and a 10 kW laser pulse at 246 GHz, the electromagnetic power generated by the acoustic echo and arriving at the detector is 1.4×10^{-18} N^4 W. The electromagnetic power at the detector would exist in a bandwidth determined by the finite number of superlattice periods given by $\Delta f = \sqrt{2}(246)/N$ GHz. For this bandwidth, the Schottky sensitivity is 3.5×10^{-8}/N W. In terms of the number of periods; the expected SNR is 4×10^{-11} N^5. For example, one would need to use a superlattice containing approximately 500 periods, corresponding to a bandwidth of 0.70 GHz, in order to achieve a SNR of 30 dB. If necessary, the SNR could be increased by the integration of successive pulses.

4.2 Ensuring specular reflection at DSL/liquid helium interface

A technical challenge would exist in producing specular reflection at the rear silicon/liquid helium interface. Specular scattering does not normally occur at ordinary (imperfect) interfaces in the case of phonons with wavelengths of a few hundred angstroms or less; instead, the scattering becomes diffusive. A strong connection exists between the defect-induced diffuse scattering of high-frequency phonons at a solid/liquid helium interface and the Kapitza effect[36] (The Kapitza effect refers to the anomalously low interfacial thermal resistance that exists between solids and liquid helium at these frequencies compared to the predictions of the acoustic impedance mismatch model.) However, work on the polarization dependence of the Kapitza effect for nearly normally incident phonons provides strong evidence that, for properly *ex situ* prepared surfaces, only the transverse modes behave anomalously.[37] For instance, a specialized wafer polishing technique, HF spin-etching, has been demonstrated to eliminate diffusive scattering for normally incident LA phonons of somewhat longer wavelength (46 GHz). The spin-etch removed the native oxide layer in such a way that the resulting surface consists of large, atomically smooth, H-terminated silicon terraces. Smooth, clean surfaces produced in this manner were reported to result in a reduction in the anomalous Kapitza transmission by a factor of 20 for 200 GHz TA phonons, compared to more conventional *ex situ* cleaning techniques, employing only detergents and/or organic solvents. In addition, laser annealing has been shown to eliminate diffusive phonon scattering at a silicon-liquid helium interface[38]. These techniques for eliminating diffusive scattering are expected to hold for higher frequency phonons as

well, provided that $q_{\perp}d<<1$, where d is the thickness of the surface defect layer, including the mean amplitude of any surface roughness, and $q_{\perp}$ is the component of the phonon wavevector normal to the surface. With increasing $q_{\perp}$, the defects extend beyond the phonon amplitude node at the surface and begin to feel the strain field. For 246 GHz LA phonons in Si, $q_{\perp} = 0.018$ A^{-1}. Any surface roughness, contaminants, defects and/or subsurface damage should therefore have a characteristic thickness much less than 50 A in order for the Kapitza anomaly to become extinguished. With recent improvements in superpolishing[34] and these surface preparation techniques, this constraint may be able to be satisfied.

4.3 Anti-reflection multilayer for terahertz LA phonons

After successful pulse-echo experiments within the crystalline substrate are completed, the next step would be to successfully transmit a coherent phonon beam into low-temperature liquid helium-4, the coupling fluid for a reflection acoustic microscope application. It would be also be necessary to apply a phonon anti-reflection coating after excimer laser-annealing rear surface of the DSL substrate for efficient and coherent phonon transmission into the liquid helium bath.

The anti-reflection multilayer for LA phonons will be fabricated using an amorphous *(a-)* silicon dioxide/silicon superlattice (ASL); the ASL has been reported by Koblinger *et al*[39]. For phonons propagating along a crystal symmetry direction and arriving at normal incidence upon a flat ASL, the anisotropy of the elastic constants may be ignored. In this case, the characteristic matrix method of stratified media[40] of classical optics may be used to compute the phonon transmissivity, provided one substitutes for the impedance of the electromagnetic wave, the acoustic impedance $Z_i = \rho v_i$ of the individual layers of the ASL with density ρ, and phonon velocity v_i .The speed of 246 GHz phonons in helium-4 is 189 m/s and the density at 150-mK is 0.145 g/cm^3 [41]. The corresponding acoustic impedance of helium-4 at this temperature becomes 2.74 x 10^3 $g/(cm^2\text{-}s)$. The ASL would be fabricated in an ultrahigh-vacuum, electron beam evaporation system as was done by Koblinger. In general, the elastic constants for amorphous materials depend upon the growth technique. However, for films grown in an ultrahigh vacuum ($<10^{-8}$ Torr) electron beam evaporation system, the impedances are known. The longitudinal phonon velocity[42], in this frequency regime, in *a*:$Si0_2$, is 5840 m/s. The density of *a*:$Si0_2$ is 2.3 g/cm^3, yielding an acoustic impedance of 1.34 x 10^6, in the above units. For *a*:Si, the longitudinal phonon velocity can be found from the TA phonon velocity, given by Koblinger, when one makes use of the simplifying assumption[43] that the TA and LA phonon velocities scale by a common factor $r = v_{TA}/v_{LA} = 0.62$. For *a*:Si in the units above, the acoustic impedance for longitudinal phonons becomes 1.64 x 10^6. Using these parameters, a simple calculation, employing the characteristic matrix method of stratified media[44], predicts a phonon transmissivity greater than 99% for a multilayer stack consisting of 32 alternating quarter-wave layers of *a*:$Si0_2$ and *a*:Si of thickness' 5.0 and 8.6 nanometers, respectively. The layer thickness can be controlled to better than 3% using *in situ* atomic absorption techniques during thin film deposition[45].

To obtain a smooth silicon/ASL interface, the *ex situ* spin-etch surface cleaning and passivation technique would be done on the superpolished and excimer laser-annealed substrate within one hour prior to the growth of the ASL. In addition, one would spin-etch the ASL surface, just prior to sample insertion into the low temperature cryostat, in order to remove a protective capping *a*:$Si0_2$ layer grown during ASL fabrication. After the capping layer had been removed, the top *a*-Si layer of the ASL would be smooth and clean[46]. By these techniques, it might be possible to eliminate the

diffusive scattering of nearly-normal incident LA phonons at the ASL/liquid helium interface and, therefore, preserve the spatial coherence of the phonon pulse as it is transmitted into the He II bath.

Santos *et al.* [47] have reported that phonons with a frequency as high as 600 GHz can easily traverse a large number (>200) of layers and interfaces of amorphous Si:H and Si:N_x without noticeable degradation. This implies that the coherence length of the phonons far exceeded the superlattice thickness (~1 μm) used by Santos. Since the ASL reported by Koblinger *et al.* has sharper filter characteristics than similar superlattices formed of amorphous Si:H and Si:N_x, one may conclude that the thickness of an amorphous Si/$Si0_2$ superlattice consisting of 32 layers should be much less than the coherence length of 246 GHz LA phonons.

In this step in the development of the THz cryogenic acoustic microscope, at some distance from the substrate in the helium-4 bath, the propagating phonon pulse would arrive normally incident upon a polished sapphire surface and undergo specular reflection[31]. A piezomotor-driven positioner specifically designed for use in low temperature applications[48] would drive the sapphire phonon mirror. It may be most prudent to perform this experiment at the University of California-Santa Barbara *Center for Terahertz Science and Technology* (available resources include a free electron laser as a tunable source of intense pulsed THz radiation (~10-KW peak power with 40-ns pulsewidth), a dilution refrigerator and fast THz detectors).

4.4 Acoustic lens

The final experiment to demonstrate the feasibility of a terahertz cryogenic acoustic microscope would be to fabricate a high-quality acoustic microlens on the rear silicon substrate and to apply the phonon anti-reflection coating as described above, to focus the phonon beam to a nanometer waist in the low-temperature helium-4. Acoustic lenses suitable for operation at a lower frequency of 1-GHz have been fabricated by an isotropic chemical etch[49]. However at terahertz frequencies, advanced dry etching techniques would be used to fabricate the precision acoustic microlens. For instance, MEMS Optical Inc. (http://www.memsoptical.com) can fabricate mm-diameter hemispherical acoustic lens with ~mm focal lengths, using gray scale technology and deep reactive ion etching, with a spherical error under 15 nm rms and a surface roughness of ~2-8 nm. Alternatively, one could attempt the fabrication of the acoustic microlens in single crystal silicon using ultra-precision lathe single-point diamond turning (Corning NetOptix, Inc., http://www.corningnetoptix.com/). Prior to the application of the phonon AR coating upon the lens surface, an excimer laser anneal[50] to remove any subsurface amorphous regions, would also be performed.

In order to accurately predict the profile of the acoustic beam waist at the focus, one would first need to calculate the spatial distribution of the transmitted phonon intensity across the surface of the AR-coated acoustic lens. The [100] phonons, propagating in the silicon substrate, will arrive at oblique angles to the convex surface of the ASL forming the AR-coating and consequently, will undergo mode conversion at the ASL interfaces. However, the calculation should be possible using recent techniques.[51]

ACKNOWLEDGEMENTS

This work has been generously supported by the US Army Research Office: Program of *Theoretical Physics and Nonlinear Phenomena*, under contract numbers DAAD19-01-1-0466 and DAAHO4-96-1-0401.

REFERENCES

1 J. Ilukor and E.H. Jacobson, “Coherent Elastic Wave Propagation in Quartz at Ultramicrowave Frequencies”, in Physical Acoustics, vol. V, W.P. Mason, Ed. (New York: Academic, 1968) p. 221-231.

2 W.E. Bron, M. Rossinelli, Y.H. Bai and F. Keilmann, “Surface requirements for piezoelectric generation of high-frequency phonons”, Phys. Rev. B 27, 1370 (1983).

3 B.C. Daly, N.C.R. Holme, T. Buma, C. Branciard, and T.B. Norris, “Imaging nanostructures with coherent phonon pulses”, Applied Physics Letters 84 (25), 5180 (2004); P. Basseras, G.M. Gracewski, G.W. Wicks, and R.J.D. Miller, “Optical generation of high-frequency acoustic waves in GaAs/AlxAlGa1-x periodic multilayer structures”, J. Appl. Phys. 75 (6), 2761 (1994); for a review, see Holger T. Ghahn, Humphrey J. Maris, and Jan Tauc, “Picosecond Ultrasonics, IEEE Journal of Quant. Electron. QE 25, 2562 (1989); H.N. Lin, R.J. Stoner, and H.J. Maris, “Picosecond Ultrasonics”, J. Nondestructive Eval. 9, 239 (1990).

4 A.J. Kent, N.M. Stanton, L.J. Challis, and M.Henini, “Generation and propagation of monochromatic acoustic phonons in gallium arsenide”, Appl. Phys. Lett. 81 (18), 3497 (2002); N.M. Stanton, C.E. Martinez, A.J. Kent, S.V. Novikov, C.T. Foxon, “Phonon generation by femtosecond pulsed laser excitation of an aluminum nitride/gallium nitride superlattice”, Phys. Stat. Sol. C 1, 2678 (2004).

5 P. Ruden and G.H. Dohler, “Anistropy Effects and Optical Excitation of Acoustic Phonons in n-i-p-i Doping Superlattices”, Solid State Commun. 45 (1), 23 (1983); J.J. Quinn, U. Strom, And L.L. Chang, “Direct Electromagnetic Generation of High Frequency Acoustic Waves in Semiconductor Superlattices”, Solid State Commun. 45, 111(1983); K. Dransfeld, “Quantum Aspects of Rayleigh Waves: Surface- and Interface-Waves at Very High Frequencies”, in Rayleigh-Wave Theory and Applications, edited by E.A. Ash and E.G.S. Paige (Springer, Berlin, 1985), p. 10; T.E. Wilson, “Proposal for the direct electromagnetic generation of coherent terahertz acoustic phonons in semiconductor superlattices at the University of California, Santa Barbara far-infrared free-electron laser facility”, JOSA B6, 1058 (1989).

6 M.S. Muha, A.A. Moulthrop, and G.C. Kozlowski, “Acoustic microscopy at 15.3 GHz in pressurized superfluid helium”, Appl. Phys. Lett. 56 (11), pp. 1019-1021, (1990); B. Hadimioglu and J.S. Foster, “Advances in Superfluid Helium Acoustic Microscopy”, J. Appl. Phys. 56, 1976 (1984).

7 Alexei A. Maradudin, “Phonon Physics - A Survey”, in Physics of Phonons, edited by T. Paszkiewicz, Series 285 of the Lecture Notes in Physics Series, (Springer-Verlag, Berlin, 1988), pp. 1-49.

8 T.E. Wilson, “Proposal for the direct electromagnetic generation of coherent terahertz acoustic phonons in semiconductor superlattices at the University of California, Santa Barbara far-infrared free-electron laser facility”, JOSA B6, 1058 (1989).

9 Gottfried H. Dohler, “The Physics and Applications of n-i-p-i Doping Superlattices”, in CRC Critical Reviews in Solid State and Materials Sciences 13, pp. 97-141 (1989).

10 E.F. Schubert, T.D. Harris, J.E. Cunningham and W. Jan, “Quantum-confined interband absorption in GaAs sawtooth-doping superlattices”, Phys. Rev. B 38, 8305 (1988).

11 W.J. Li, B.D. McCombe, “Coupling efficiency of metallic gratings for excitation of intersubband transitions in quantum-well structures”, J. Appl. Phys. 71 (2) 1038 (1992); M. Helm, E. Colas, P. England, F. DeRosa, and S.J. Allen, Jr., “Observation of grating-induced intersubband emission from GaAs/A1GaAs superlattices”, Appl. Phys. Lett. 53, 1714 (1988); Y. Wang and S. Li, “A numerical analysis of the double periodic reflection metal grating for multiquantum well infrared photodetectors”, J. Appl. Phys. 74, 2192 (1993).

12 K. Winer and M. Cardona, “Theory of infrared absorption in silicon”, Phys. Rev. B 35 (15) 8189 (1987).

13 L. Genzel, Chapter 15, “Impurity-Induced Lattice Absorption”, in Optical Properties of Solids (Plenum Press, NY 1969) pp. 453-487; L. Genzel, K.F. Renk, and R. Weber, “Calculation of Impurity-Induced Lattice Mode Absorption”, Phys. Stat. Sol. 12, 639 (1965); W.M. Dennis, “Investigations of Nonequilibrium Phonons Using Defect-Induced One-Phonon Absorption”, in Phonon Scattering in Condensed Matter VII, ibid., pp. 121-122.

14 John Paul Turneaure, “Microwave Measurements of the Surface Impedance of Superconducting Tin and Lead”, Stanford University Ph.D. thesis 1967, University Microfilms 67-17, 517 (Ann Arbor, MI).

15 Maria Schwarte and Paul Berberich, “Piezo phonon spectroscopy of the ground states of acceptors in Si and Ge”, J. Phys. C: Solid State Phys. 18, 3225 (1985); Helmut Kinder, Monochromatic Phonon Generation by Superconducting

Tunnel Junctions", Nonequilibrium Phonon Dynamics, NATO ASI Series B: Physics Volume 124 (Plenum Press, New York, 1985) pp. 129-164.
16 S.C. Edwards, Hamid bin Rani, and J.K. Wigmore, "The use of superconducting bolometers for detecting nanosecond heat pulses", J. Phys. E: Sci. Instrum. 22, 582 (1989); GA. Northrop and J.P. Wolfe, "Phonon Imaging: Theory and Applications", in Nonequilibrium Phonon Dynamics, ibid, pp. 165-234.
[17] 17 D. Froehlich and W. Nieswand, "Nonlinear optics of CuCl under uniaxial stress", Philosophical Magazine B 70 (3), 321 (1994).
[18] M.P. Hacker, Z. Drozdowicz, D.R. Cohn, K. Isobe, and R.J. Temkin, "A High Power, 1.22 mm $^{13}CH_3F$ Laser", Physics Letters 57A (4), 328 (1976).
[19] T.E. Wilson, "Preliminary Results Using a Far-Infrared Laser Cavity-Dumper", Bulletin of APS 32, no.2, B1O, 328 (1987); T.E. Wilson, "A High-Power Millimeter Wave 13CH3F Laser Pumped in a Three Mirror CO2 Laser Cavity with Optically-Switched Cavity-Dumping", post-deadline paper delivered at the 13th Imt. Conf. Infrared and Millimeter Waves, Honolulu, 5-9 Dec. 1988; T.E. Wilson, "A Compact High-Power FIR Laser Pumped in a Three Mirror CO2 Laser Cavity with Semiconductor-Switched Cavity-Dumping", in U.S. Department of Energy Strategic Defense Initiative's New and Innovative Concepts Program Summary Report, edited by R. LeChevalier, (TPI Publishing, Falls Church, VA, 1989), pp. 79-80; Thomas E. Wilson, "Modeling the high-speed switching of far-infrared radiation by photoionization in a semiconductor", Phys. Rev. B 59 (20), 12996 (1999).
[20] R.E.M. de Bekker, L.M. Claessen, and P. Wyder, "Generation of very short far-infrared pulses by cavity dumping a molecular gas laser", J. Appl. Phys. 68, 3729 (1990); J.P. Kaminski, J.S. Spector, C.L. Felix, D.P. Enyeart, D.T. White, and G. Ramian, "Far-infrared cavity dump coupling of the UC Santa Barbara free-electron laser", Appl. Phys. Lett. 57, 2770 (1990); J. Burghoorn, J.P. Kaminski, R.C. Strijbos, T.O. Klaassen, and W. Th. Wenckebach, "Generation of subnanosecond high-power far-infrared pulses by using a passive resonator pumped by a free electron laser", J. Opt. Soc. Am. B 9, 1888 (1992).
[21] Design courtesy of Paul Woskov, Associate Head, Plasma Technology Division, Plasma Science and Fusion Center, MIT, 77 Massachusetts Avenue, Cambridge, MA 02139-4307
[22] Coherent Inc.,5100 Patrick Henry Drive, Santa Clara, CA 95054 USA
[23] Roger W. Cohen and B. Abeles, "Superconductivity in Granular Aluminum Films", Phys. Rev. 168 (2), 444 (1967).
[24] Daniel L. Meier, John X. Przybysz and Joonhee Kang, "Fabrication of an all-refractory circuit using lift-off with image-reversal lithography", IEEE Trans. Magnetics 27 (2) 3121 (1991); Product Data Sheet "AZ 5214 E Image Reversal Photoresist", AZ Electronic Materials, 70 Meister Avenue, Somerville, NJ 08876
[25] SUSS MicroTec Inc., 228 SUSS Drive, Waterbury Center, VT 05677-0157; Adtek Photomask 4950 Fisher Street Montreal, QC H4T 1J6 CANADA; Tanner Research, 2650 East Foothill Boulevard, Pasadena, CA 91107
26 Denton Vacuum, 1259 North Church St., Moorestown, NJ 08057
27 H. Preston-Thomas, The International Temperature Scale of 1990 (ITS-90), *Metrologia* 27, 107 (1990).
28 P. Berberich and Maria Schwarte, "Phonon Emission Spectra of Superconducting Tunnel Junctions", Z. Phys. B – Condensed Matter 64, 1 (1986).
[29] Model 153 lapping and polishing fixture with custom mounting block from South Bay Technology Inc., 11120 Via Callejon, San Clemente, CA 92673.
30 Viertl, J.R.M., 1973, Ph.D. Thesis, Cornell University.
31 G.A. Northrop and J.P. Wolfe, "Phonon reflection imaging: A determination of specular versus diffuse boundary scattering", Phys. Rev. Lett. 52, 2156 (1984).
32 K. Karaki, T. Saito, K. Matsumoto, and Y. Okuda, "Nonlinear resolution improvement and second-harmonic generation of a pressurized superfluid 4He acoustic microscope", Appl. Phys. Lett. 59, 908 (1991).
33 M A H Tucker and A F G Wyatt, "Four-phonon scattering in superfluid 4He", J. Phys. Condens. Matter 4 7745 (1992); Humphrey J. Maris, "Phonon-phonon interactions in liquid helium", Rev. Mod. Phys. 49, 341 (1977); R.C. Dynes and V. Narayanamurti, "Measurement of the anomalous dispersion and the excitation spectrum of He II, Phys. Rev. B 12, 1720 (1975).
34 Silicon superpolished substrates, when characterized by a Micromap Promap 512 profiler with a noise floor of 0.01-nm, are found to have rms surface micro-roughness and flatness of only 0.05-nm over millimeter-sized areas. Research Electro-Optics, Inc., 1855 South 57th Street, Boulder, CO 80301.
35 Millitech, Inc., South Deerfield, MA.
[36]E.T. Swartz and R.O. Pohl, "Thermal Boundary Resistance", Rev. Mod. Phys. **61** (3), 605 (1989).

37 H. Kinder, A. De Nmnno, D. Goodstein, G. Paterno, F. Scaramuzzi, and S. Cunsolo, "Extinction of the Kapitza anomaly for phonons along the surface normal direction", Phys. Rev. Lett. 55, 2441 (1985).
38 L. Loester, A. Colli, S. Wurdack, W. Dietsche, and H. Kinder, "Resonant scattering of phonons by adsorbates on clean silicon surfaces", Z. Phys. B – Condensed Matter 80, 275 (1990); W. Eisenmenger, "Phonon Scattering at Surfaces and Interfaces", Phonon Scattering in Cond. Matter V (Springer Series Solid State Sciences 68) 204, 1986.
[39] 0. Koblinger, J. Mebert, S. Dittrich, S. Dottinger, and W. Eisemnenger, "Phonon Stop Bands in Amorphous Superlattices", Phys. Rev. B **35**, 9372 (1987); V. Narayanamurti, H.L. Stormer, M.A. Chin, A.C. Gossard, and W. Wiegmann, "Selective Transmission of High-Frequency Phonons by a Superlattice: The 'Dielectric Phonon Filter' ", Phys. Rev. Lett. **43**, 2012 (1979).
40 Max Born and Emil Wolf, Principles of Optics, 6th edition, (Pergammon Press, New York 1980), p. 70.
41 Ruslan V. Vovk, Charles D.H. Williams, and Adrian F.G. Wyatt, "High-energy phonon pulses in liquid 4He", Phys. Rev. B 69 , 144524 (2004); Russell J. Donnelly and Carlo F. Barenghi , "The Observed Properties of Liquid Helium at the Saturated Vapor Pressure", http://darkwing.uoregon.edu/~rjd/vapor1.htm
42 M. Rothenfusser, W. Dietsche, and H. Kinder, "Phonon-Dispersion Measurements in Glasses", Phonon Scattering in Condensed Matter, ibid, pp. 419-421.
43 P.V. Santos, L. Ley, J. Mebert and 0. Koblinger, "Experimental evidence for couple-mode phonon gaps in superlattice structures", Phys. Rev. B 36, 1306 (RC) (1987); P.V. Santos and L. Ley, "Phonons in Amorphous Superlattices", Superlattices and Microstructures 5, 43 (1989).
44 Also see, H. Kato, "Transmission of L-mode phonons from a superlattice into a liquid by effective acoustic impedance matching", Phys. Rev. B 59, 11136 (1999); Eric L. Adler, "Matrix Methods Applied to Acoustic Waves in Multilayers", IEEE Trans. On Ultrasonics, Ferroelectrics and Frequency Control 37(6), 485 (1990).
45 Personal communication from Peter Chow of Superior Vacuum Technology Associates, Inc., 7620 Executive Drive, Eden Prairie, MN 55344. See also, Charles M. Falco, "Growth of metallic and metal containing superlattices", Chapter 1 in Physics Fabrication and Application of Multilayer Structures, edited by P. Dhez (Plenum Press, NY) 1988.
46 It has been reported that HF solutions do not etch silicon substrates. Thus, the etch acting upon Si/S102 leaves the Si substrate the same as the former Si/Si02 interface; U. Newwald, H.E.. Hessel, A. Feltz, U. Memmert, and R.J. Behm, "Wet chemical etching of Si(100) surfaces in concentrated NH4F solution: formation of (2X1)H reconstructed Si(100) terraces versus (111) facetting", Surface Science Letters 296, L8 (1993).
47 P.V. Santos, L. Ley, J. Mebert and 0. Koblinger, "Frequency gaps for acoustic phonon in a:Si:H/a:SiNx:H superlattices", Phys. Rev. B 36, 4548 (1987).
48 I.B. Altfeder, and A.P. Volodin, "Low-temperature scanning tunneling microscope with a reliable piezoelectrical coarse-approach mechanism", Rev. Sci. Instrum. 64, 3157 (1993).
49 H. Hashimoto, S. Tanaka, and K. Sato, "Silicon acoustic lens for scanning acoustic microscope (SAM)", Jap. J. Appl. Phys., Part 1, 32, 5B, 2543 (1993).
50 Y. P. Zeng, Y F Lu, Z X shen, W X Sun, T Yu, L Liiu, J N Zeng, B J Cho, and C H Poon, "Raman spectroscopy investigation on excimer laser annealing and thickness determination of nanoscale amorphous silicon", Nanotechnology 15, 658 (2004).
51 S. Tamura, D.C. Hurley and J.P. Wolfe, "Acoustic-phonon propagation in superlattices", Phys. Rev. B 38, 1427 (1988); M.J. Kelly, "Acoustic phonon transmission in superlattices", J. Phys. C: Solid State Phys. 18, 5963 (1985); 0. Weiss, Z. Phys. B34, 55 (1979).